Two-center convergent-close-coupling calculations of positron scattering on magnesium

R. Utamuratov,* D. V. Fursa, A. S. Kadyrov, A. V. Lugovskoy, J. S. Savage, and I. Bray
ARC Centre for Antimatter-Matter Studies, Department of Applied Physics, Curtin University, Perth 6152, Australia
(Received 15 October 2012; published 7 December 2012)

The two-center convergent-close-coupling method is extended to the calculation of positron scattering from atoms with two valence electrons above an inert ion core. Calculations of positron scattering on magnesium have been performed over a wide energy range. Elastic scattering, Positronium formation, target excitation, and direct ionization cross sections have been calculated. Results are in reasonably good agreement with the experimental data where available. Current results confirm the existence of a low-energy shape resonance predicted by variational and single-center convergent-close-coupling methods.

DOI: 10.1103/PhysRevA.86.062702 PACS number(s): 34.80.Uv, 34.80.Lx

I. INTRODUCTION

The positron, as the simplest antimatter particle, has been a major subject of matter-antimatter interaction studies since its discovery. Recent advances in positron-beam technologies and their broad applications as a diagnostic tool have further increased the need for deeper understanding of positron interactions with atoms. The theoretical description is challenging due to the two-center nature of the problem. This two-center nature arises from the fact that a positron, being positively charged, can capture an electron from the target atom thereby forming positronium (Ps). The two centers require a mix of coordinate systems, leading to a very complex underlying theory. In particular, a rigorous inclusion of electron exchange between Ps and the residual ion remains an unsolved problem. Experiments are also difficult due to the requirement of obtaining positron beams with sufficient energy resolution and intensity.

So far, only the Detroit group at Wayne State University has reported experimental data for e^+-Mg scattering [1–3]. Total scattering cross sections have been measured for incident energies between 2 and 50 eV [1,2]. Upper and lower limits for Ps-formation cross sections have been reported in Ref. [3] for positron incident energies of 0.1–60 eV. Both results have been regarded as preliminary because of large uncertainties arising from difficulties associated with the use of the magnesium target.

Various theoretical approaches have been applied to the e^+-Mg scattering problem. Szmytkowski [4] has calculated the elastic-scattering cross section by using the polarized orbital method (POM). However, the results were not in agreement with experiments. Campeanu *et al.* [5] calculated the total scattering cross section at intermediate and high energies by combining the elastic cross section obtained within the POM with inelastic cross sections calculated using a distorted wave approximation. Their results agree with the experimental data above 30 eV but significantly underestimate the experiment at lower energies. Gribakin and King [6] applied the many-body Green's function theory method to the problem by accounting for the Ps formation on its ground state. Although their results were not in good agreement with the experiment [1], they showed the significance of the Ps-formation channels even below the Ps-formation threshold. Calculations by Ryzhikh *et al.* [7], using the stochastic variational principle, predicted that positrons may bind to Mg with a binding energy of 0.373 eV. Bromley *et al.* [8] have tuned free parameters of the POM model to replicate this predicted positron binding energy and then calculated the elastic cross section, phase shifts, and scattering lengths at low energies. The results for the total scattering cross section were broadly consistent with the experimental data. Hewitt *et al.* [9] performed two-center close-coupling- (CC-)type calculations by using the two lowest states of Mg and the three lowest states of Ps. The Mg states have been obtained within an independent particle model, which effectively treats Mg as a single-electron target. The results for the total cross section, obtained as a sum of cross sections of all included channels, were in poor agreement with the experiment of Stein *et al.* [1]. As cited by Surdutovich *et al.* [3], Walters calculated the Ps-formation cross section using the two-center method, which was developed for helium by Campbell *et al.* [10]. Cheng and Zhou [11] have used the optical-model approach, which uses a complex equivalent-local polarization potential to calculate Ps formation in ground and $2s$ and $2p$ excited states. Their result for the total Ps-formation cross section agrees reasonably well with the experimental data of Surdutovich *et al.* [3] but differs from results of close-coupling [9] and many-body [6] calculations.

Mitroy *et al.* [12] applied the configuration interaction (CI) method to generate low-energy phase shifts for elastic scattering using bound-state calculations to the problem of e^+-Mg scattering. The semiempirical optical potential has been fine-tuned by using a large configuration interaction calculation. The Ps-formation channels have been indirectly accounted for via the use of a very large CI expansion with high orbital angular momenta states. They predicted a P-wave resonance at about 0.1-eV positron scattering energy.

Recently, the single-center convergent-close-coupling (CCC) method has been applied to the e^+-Mg scattering problem by Savage *et al.* [13]. The single-center method can give accurate results below the Ps-formation threshold and above the ionization threshold by utilizing a large basis, which includes high orbital angular momentum states. However, it cannot explicitly calculate the Ps-formation cross sections and, therefore, is not applicable in the energy region between the Ps-formation and the ionization thresholds. The elastic-scattering phase shift, target excitation, and total ionization (which implicitly contains Ps-formation) cross sections have

*r.utamuratov@curtin.edu.au

been calculated. The elastic-scattering phase shift and cross section were in good agreement with the results of Mitroy *et al.* [12]. The approach also showed the existence of the P-wave resonance, however, with a slightly different position (0.15 vs 0.1 eV) and magnitude than the one predicted by Mitroy *et al.* [12].

One of the interesting features of positron interactions is the attachment to atoms and molecules [6,7,12]. Experiments can indirectly show whether there are such bound states through accurate measurements of elastic scattering at very low collision energies. By having good agreement between such measurements and calculations, the existence of positron binding can be indirectly verified.

The purpose of this paper is to provide the most accurate and complete theoretical results for positron scattering on magnesium. To do so, we include the Ps-formation channels in the corresponding CCC formalism, yielding a valid method over the entire energy range with explicit results for Ps formation.

II. FORMALISM

A. Mg structure

We model Mg as a system with two active electrons above a frozen Hartree-Fock core [14,15]. The interaction V_e between an active electron and the frozen Hartree-Fock core is calculated as a static part of the Hartree-Fock potential V_{st} plus an exchange potential V_{ex} between an active and the core electrons,

$$V_e(r) = V_{st}(r) + V_{ex}(r). \tag{1}$$

The static part of the Hartree-Fock potential V_{st} is calculated as

$$V_{st}(r) = -\frac{Z}{r} + 2\sum_{\psi_j \in C} \int d^3r' \frac{|\psi_j(\boldsymbol{r}')|^2}{|\boldsymbol{r} - \boldsymbol{r}'|}, \tag{2}$$

where Z is the charge of the nucleus and ψ_j are the states of the ion core C generated by performing the self-consistent-field Hartree-Fock calculations [16]. The summation in Eq. (2) is performed for all core electron pairs.

Previously, single-center CCC calculations of e^+-Mg [13] and e^--Mg [14,15] problems have used nonlocal Hartree-Fock exchange between an active electron and the core electrons. In this paper, however, the exchange between the active electron and the core electrons is taken into account in the framework of the equivalent local-exchange approximation [17],

$$V_{ex}(r) = \tfrac{1}{2}\{[E_{ex} - V_{st}(r)] - \sqrt{[E_{ex} - V_{st}(r)]^2 + \rho(r)}\}, \tag{3}$$

where

$$\rho(r) = \sum_{\psi_j \in C} \int d\hat{\boldsymbol{r}} |\psi_j(\boldsymbol{r})|^2 \tag{4}$$

is the electron-density distribution in the core and E_{ex} is some free adjustment parameter. This parameter is chosen to get the correct ground-state energy. The reason for such an approximation is to avoid the complexities arising from the use of nonlocal potentials in calculating the rearrangement matrix elements. The applicability of the approximation has been tested by performing the single-center e^+-Mg calculations and obtaining an excellent agreement with the results of Savage *et al.* [13].

A set of one-electron orbitals $\{\varphi_{nl}\}$ is obtained via diagonalization of the Mg^+ Hamiltonian in a Sturmian (Laguerre) basis,

$$\xi_{nl}(r) = \sqrt{\frac{\lambda_l (n-1)!}{(2l+1+n)!}} (\lambda_l r)^{l+1} \exp(-\lambda_l r/2) L_{n-1}^{2l+2}(\lambda_l r), \tag{5}$$

where λ_l are exponential fall-off parameters and

$$L_{n-1}^{2l+2}(x) = \sum_{m=0}^{j} \frac{(-1)^m (j+n)!}{(j-m)!(n+m)!m!} x^m \tag{6}$$

are the associated Laguerre polynomials, l is the angular momentum, and n ranges from 1 to the basis size N_l. The exponential fall-off parameters were chosen to be $\lambda_l = 3.0$. The maximum value of angular momentum l_{max} together with the values of N_l will ultimately determine the size of the target basis used in the scattering calculations and will be the subject of convergence studies.

The one-electron orbitals $\{\varphi_{nl}\}$ are used to form a set of antisymmetric two-electron configurations, followed by standard CI calculations of the Mg wave functions. The calculated Mg states $\{\psi_\alpha^{(N)}\}$, $\alpha = 1, \ldots, N$, diagonalize the Mg target Hamiltonian H_T,

$$\left\langle \psi_{\alpha'}^{(N)} \middle| H_T \middle| \psi_\alpha^{(N)} \right\rangle = \epsilon_\alpha^{(N)} \delta_{\alpha'\alpha}, \tag{7}$$

where ϵ_α are the (pseudo)state energies. The target (pseudo)states $\psi_\alpha^{(N)}$ are expressed via two-electron configurations as

$$\psi_\alpha^{(N)}(\boldsymbol{r}_1, \boldsymbol{r}_2) = \sum_{ab}^{N} C_{ab}^{\alpha} \sum_{l_a, m_a, l_b, m_b} C_{l_a m_a l_b m_b}^{lm} \varphi_a(\boldsymbol{r}_1) \varphi_b(\boldsymbol{r}_2), \tag{8}$$

where the CI coefficients C_{ab}^{α} satisfy the symmetry property,

$$C_{ab}^{\alpha} = (-1)^{S + l_a + l_b - l} C_{ba}^{\alpha}$$

to ensure antisymmetry of the two-electron target states. The orbital and spin angular momenta are denoted by l and S, respectively. The lowest-energy states are good approximations of the Mg bound eigenstates, whereas, the higher-energy pseudostates provide for a discretization of the target continuum.

Note that, for positron scattering on the ground state of magnesium, only states with $S = 0$ are required. Table I shows the ionization energies from the lowest singlet ($S = 0$) states

TABLE I. Ionization energies of Mg singlet states in eV.

State	$N_0 = 16$	$N_0 = 22$	Experiment
$3S$	7.642	7.642	7.646
$3P$	3.241	3.241	3.300
$3D$	1.863	1.889	1.893
$4S$	1.185	2.244	2.253
$4P$	1.221	1.471	1.528
$4D$	0.531	0.910	1.058
$4F$	0.281	0.706	0.867

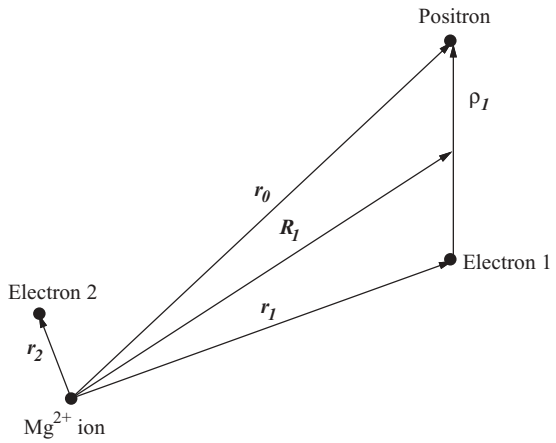

FIG. 1. Coordinate system for e^+-Mg scattering.

of Mg obtained with $N_0 = 16$ and $N_0 = 22$. From the table, one can see that the ground and $3P$ (the first excited) states have converged very close to the real eigenvalues, whereas, the other lowest excited states get closer to the real eigenvalues as basis size is increased.

B. Scattering

Since we model Mg as a He-like target, we may readily utilize the positron-helium scattering theory given earlier [18] and cover the theoretical details here more briefly.

The scattering wave function Φ must satisfy the Schrödinger equation,

$$(H - E)\Phi(\boldsymbol{r}_0,\boldsymbol{r}_1,\boldsymbol{r}_2) = 0, \tag{9}$$

where E is the total energy and H is the total Hamiltonian for this system, $\boldsymbol{r}_0$, $\boldsymbol{r}_1$, and $\boldsymbol{r}_2$ denote the positions of the positron, electron 1, and electron 2, respectively. To describe the Ps center, it is convenient to use Jacobi coordinates $(\boldsymbol{R},\boldsymbol{\rho})$, where $\boldsymbol{R} = 1/2(\boldsymbol{r}_0 + \boldsymbol{r}_1)$ is the position of the Ps center of mass (c.m.) relative to the target nucleus and $\boldsymbol{\rho} = \boldsymbol{r}_0 - \boldsymbol{r}_1$ is the relative coordinate of the positron and electron. The two systems of coordinates $(\boldsymbol{r}_0,\boldsymbol{r}_1,\boldsymbol{r}_2)$ and $(\boldsymbol{R},\boldsymbol{\rho},\boldsymbol{r}_2)$ are shown in Fig. 1. We emphasize that since there are two electrons, which can form positronium, there are two corresponding sets of Jacobi coordinates. When necessary, we will refer to them explicitly as $(\boldsymbol{R}_1,\boldsymbol{\rho}_1,\boldsymbol{r}_2)$ and $(\boldsymbol{R}_2,\boldsymbol{\rho}_2,\boldsymbol{r}_1)$. Figure 1 shows one of them where Ps is formed by electron 1.

We are interested in relatively low-energy positron collisions and so, may neglect the relativistic and spin-orbit interactions. With these assumptions, the total Hamiltonian of the e^+-Mg system can be written as

$$H = H_0 + V_e(r_1) + V_e(r_2) + V_p(r_0) + \frac{1}{|\boldsymbol{r}_1 - \boldsymbol{r}_2|} - \frac{1}{|\boldsymbol{r}_0 - \boldsymbol{r}_1|} - \frac{1}{|\boldsymbol{r}_0 - \boldsymbol{r}_2|}, \tag{10}$$

where

$$H_0 = -\tfrac{1}{2}\nabla_0^2 - \tfrac{1}{2}\nabla_1^2 - \tfrac{1}{2}\nabla_2^2$$

is the free Hamiltonian of three particles. V_e and V_p are interaction potentials between the inert ion core with an active electron and positron, respectively.

Electron interaction with the inert ion core V_e is given in Eq. (1). Positron interaction with the inert ion core is just a static part of the Hartree-Fock potential,

$$V_p(r) = -V_{st}(r), \tag{11}$$

where V_{st} is given by Eq. (2).

Following the two-center CCC approach [18,19], the scattering wave function Φ is sought as an expansion,

$$\Phi \approx \sum_{\alpha}^{N_\alpha} F_\alpha(\boldsymbol{r}_0)\psi_\alpha(\boldsymbol{r}_1,\boldsymbol{r}_2) + \sum_{\beta}^{N_\beta}\{G_\beta(\boldsymbol{R}_1)\psi_\beta(\boldsymbol{\rho}_1)\phi_{ion}(\boldsymbol{r}_2) + G_\beta(\boldsymbol{R}_2)\psi_\beta(\boldsymbol{\rho}_2)\phi_{ion}(\boldsymbol{r}_1)\}, \tag{12}$$

where the first term corresponds to expansion in terms of the magnesium wave functions ψ_α with expansion coefficients being F_α, whereas, the second term corresponds to expansion in terms of the positronium states ψ_β with coefficients G_β. N_α and N_β are the numbers of the atomic and Ps states, respectively. Indices α and β run over all included basis states of the magnesium and Ps. The basis states may contain both eigen- and positive-energy pseudostates of both Mg and Ps depending on the choice. The second term allows for both active electrons to form positronium. The residual ion of Mg^+ is described by ϕ_{ion}, and we consider it to be only in its $3s$ ground state.

Substituting the expansion (12) into (9) and following Ref. [20], we obtain momentum-space coupled-channel equations for transition matrix elements,

$$T_{\gamma'\gamma}(\boldsymbol{q}_{\gamma'},\boldsymbol{q}_\gamma) = V_{\gamma'\gamma}(\boldsymbol{q}_{\gamma'},\boldsymbol{q}_\gamma) + \sum_{\gamma''}^{N_\alpha+N_\beta}\int\frac{d\boldsymbol{q}_{\gamma''}}{(2\pi)^3} \times V_{\gamma'\gamma''}(\boldsymbol{q}_{\gamma'},\boldsymbol{q}_{\gamma''})\mathcal{G}_{\gamma''}(q_{\gamma''}^2)T_{\gamma''\gamma}(\boldsymbol{q}_{\gamma''},\boldsymbol{q}_\gamma), \tag{13}$$

where $\gamma = \alpha,\beta$ and $\boldsymbol{q}_\gamma$ is the momentum of free particle γ relative to the c.m. of the bound pair in channel γ. The effective two-body free Green's functions are defined as

$$\mathcal{G}_{\alpha''}(q_{\alpha''}^2) = \left(E + i0 - q_{\alpha''}^2/2 - \epsilon_{\alpha''}\right)^{-1}, \tag{14}$$

$$\mathcal{G}_{\beta''}(q_{\beta''}^2) = \left(E + \epsilon_{ion} + i0 - q_{\beta''}^2/4 - \epsilon_{\beta''}\right)^{-1}, \tag{15}$$

and describes the free relative motion of particle γ'' and bound pair γ'' with binding energy $\epsilon_{\gamma''}$, where ϵ_{ion} is the binding energy of the residual ion. Fundamentally, due to the nonorthogonality of the two-center expansion, the underlying equations (13) are highly ill conditioned. This requires higher accuracy in the calculations of coupled equations as the basis sizes are increased.

The effective potentials are given by

$$\begin{aligned} V_{\alpha'\alpha}(\boldsymbol{q}_{\alpha'},\boldsymbol{q}_\alpha) &= \langle\boldsymbol{q}_{\alpha'}|\langle\psi_{\alpha'}|U_{\alpha'\alpha}|\psi_\alpha\rangle|\boldsymbol{q}_\alpha\rangle,\\ V_{\beta'\beta}(\boldsymbol{q}_{\beta'},\boldsymbol{q}_\beta) &= \langle\boldsymbol{q}_{\beta'}|\langle\psi_{\beta'}\phi_{ion}|U_{\beta'\beta}|\psi_\beta\phi_{ion}\rangle|\boldsymbol{q}_\beta\rangle,\\ V_{\beta\alpha}(\boldsymbol{q}_\beta,\boldsymbol{q}_\alpha) &= \langle\boldsymbol{q}_\beta|\langle\psi_\beta\phi_{ion}|U_{\beta\alpha}|\psi_\alpha\rangle|\boldsymbol{q}_\alpha\rangle, \end{aligned} \tag{16}$$

where

$$U_{\alpha',\alpha} = V_{\rm p}(r_0) - \frac{1}{|\boldsymbol{r}_0 - \boldsymbol{r}_1|} - \frac{1}{|\boldsymbol{r}_0 - \boldsymbol{r}_2|},$$
$$U_{\beta',\beta} = V_{\rm p}\left(\left|\boldsymbol{R} + \frac{1}{2}\boldsymbol{\rho}\right|\right) - V_{\rm e}\left(\left|\boldsymbol{R} - \frac{1}{2}\boldsymbol{\rho}\right|\right) + \frac{1}{\left|\boldsymbol{R} - \frac{1}{2}\boldsymbol{\rho} - \boldsymbol{r}_2\right|} - \frac{1}{\left|\boldsymbol{R} + \frac{1}{2}\boldsymbol{\rho} - \boldsymbol{r}_2\right|},$$
$$U_{\beta,\alpha} = U_{\alpha,\beta} = H - E \tag{17}$$

are the channel potential operators.

Upon partial-wave expansion in total orbital angular momentum J according to [and similar for $T_{\gamma'\gamma}(\boldsymbol{q}_{\gamma'},\boldsymbol{q}_{\gamma})$]

$$V_{\gamma'\gamma}(\boldsymbol{q}_{\gamma'},\boldsymbol{q}_{\gamma}) = \sum_{L',M',L,M,J,K} Y_{L'M'}(\widehat{\boldsymbol{q}}_{\gamma'}) C^{JK}_{L'M'l'm'} \times \mathcal{V}^{L'LJ}_{\gamma',\gamma}(q_{\gamma'},q_{\gamma}) C^{JK}_{LMlm} Y^{*}_{LM}(\widehat{\boldsymbol{q}}_{\gamma}), \tag{18}$$

Eq. (13) transforms to

$$\mathcal{T}^{L'LJ}_{\gamma',\gamma}(q_{\gamma'},q_{\gamma}) = \mathcal{V}^{L'LJ}_{\gamma',\gamma}(q_{\gamma'},q_{\gamma}) + \sum_{\gamma''}^{N_\alpha+N_\beta} \sum_{L''} \times \int \frac{dq_{\gamma''} q^2_{\gamma''}}{(2\pi)^3} \mathcal{V}^{L'L''J}_{\gamma',\gamma''}(q_{\gamma'},q_{\gamma''}) \times G_{\gamma''}\left(q^2_{\gamma''}\right) \mathcal{T}^{L''LJ}_{\gamma'',\gamma}(q_{\gamma''},q_{\gamma}), \tag{19}$$

where L, L', and L'' are the angular momenta of the free particles in channels γ, γ', and γ'', respectively. The effective potentials in the representation of the total angular momentum are given by

$$\mathcal{V}^{L'LJ}_{\gamma',\gamma}(q_{\gamma'},q_{\gamma}) = \sum_{m',m,M',M} \iint d\widehat{\boldsymbol{q}}_{\gamma'} d\widehat{\boldsymbol{q}}_{\gamma} Y^{*}_{L'M'}(\widehat{\boldsymbol{q}}_{\gamma'}) \times C^{JK}_{L'M'l'm'} V_{\gamma'\gamma}(\boldsymbol{q}_{\gamma'},\boldsymbol{q}_{\gamma}) C^{JK}_{LMlm} Y_{LM}(\widehat{\boldsymbol{q}}_{\gamma}), \tag{20}$$

where $Y_{LM}(\widehat{\boldsymbol{q}}_{\gamma})$ are the spherical harmonics of unit vector $\widehat{\boldsymbol{q}}_{\gamma}$. The angular momenta of pair γ (γ') are l (l'), and M,m,K are the projections of L,l,J, respectively. Accordingly, $K = M + m = M' + m'$.

Note that, within this model, the main difference between e^+-Mg and e^+-He problems is that we use numerical potentials $V_{\rm e}$ and $V_{\rm p}$ instead of the pure Coulomb potentials for interactions of positrons and electrons with the nucleus. This means that the derivations of transition matrix elements are the same as for the positron-helium case, and the details can be found in Ref. [18].

III. RESULTS

Our previous calculations of positron scattering from hydrogen, helium, and alkali targets [18,19,21] have shown that better convergence is achieved when both centers are treated on equal footing by using a similar number of basis states on both centers. However, in the case of Mg, we were not able to obtain stable results when the Ps center had a similarly large number of states. This behavior might be due to the approximation, made by dropping the electron-exchange term between the Ps and the residual ion, which we adopt for positron scattering from He and He-like targets. Another possibility for such instability can be that the overcompleteness of similar near-complete double-center expansions has become more problematic than previously found for H, He, Li, and Na.

To avoid instabilities in the calculations with a large number of states from both centers, we adopt a slightly different approach. We take a complete set of target states, and then we add to it the ground state of Ps at low energies and two more eigenstates above their thresholds. This kind of expansion satisfies the scattering boundary conditions at any energy range including the area between the Ps formation and the ionization thresholds where a single-center expansion is not valid. Therefore, we should be able to get all cross sections, including Ps formation, over the full energy range of interest. We denote our results as CCC($N_{l_{\rm max}}$,$n_{\rm Ps}$), where $N_{l_{\rm max}}$ indicates the total number and the highest orbital momentum ($l_{\rm max}$) of Mg states and $n_{\rm Ps}$ is the number of Ps eigenstates.

Figure 2 shows the $J = 0$ and $J = 1$ partial-wave elastic cross sections calculated with different bases below the Ps-formation threshold (0.85 eV). It also shows the single-center results of Savage *et al.* [13], which were obtained by utilizing 305 states of Mg with the highest orbital angular momentum $l_{\rm max}$ as high as 20. Such high orbital momentum states were needed to get a convergent result within the single-center CCC. The difference between CCC(79_3,0), which does not contain

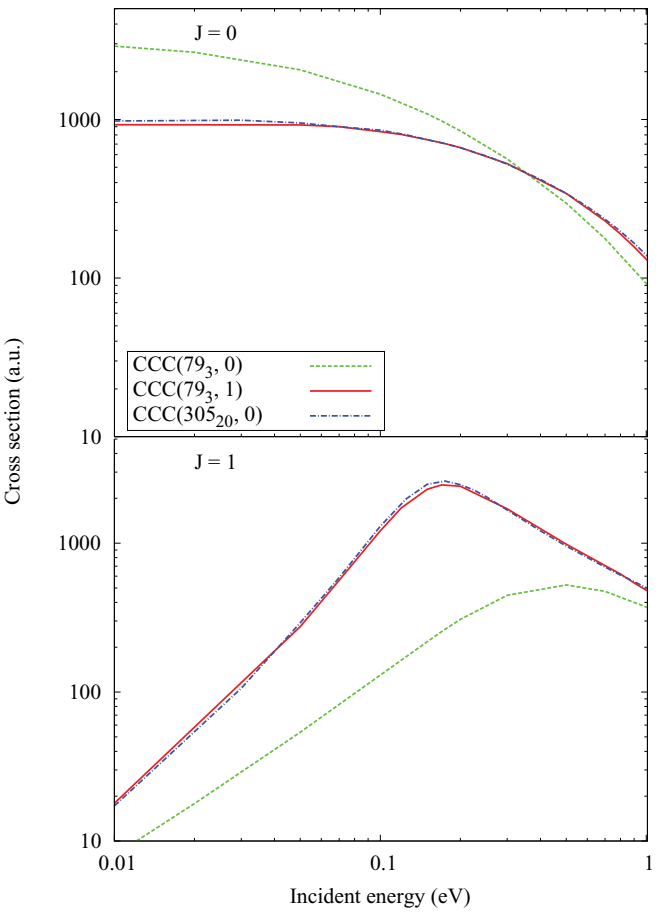

FIG. 2. (Color online) e^+-Mg elastic-scattering cross sections for the $J = 0$ and $J = 1$ partial waves. The CCC(305_{20},0) result is due to Savage *et al.* [13].

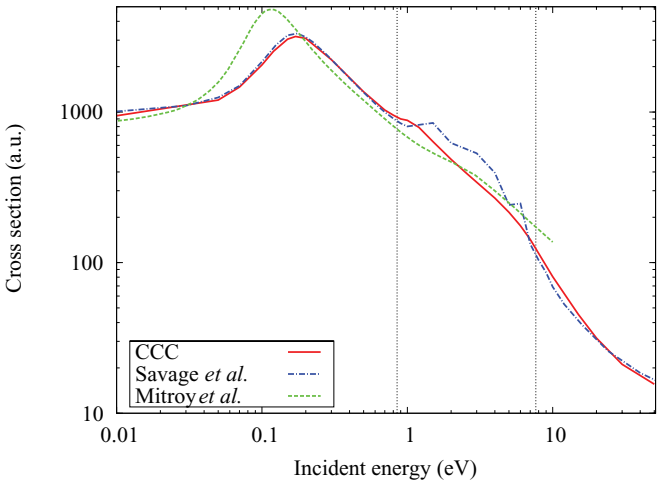

FIG. 3. (Color online) e^+-Mg elastic-scattering cross section. The first vertical line is at the Ps-formation threshold, and the second one is at the Mg-ionization threshold. Other details are given in the text.

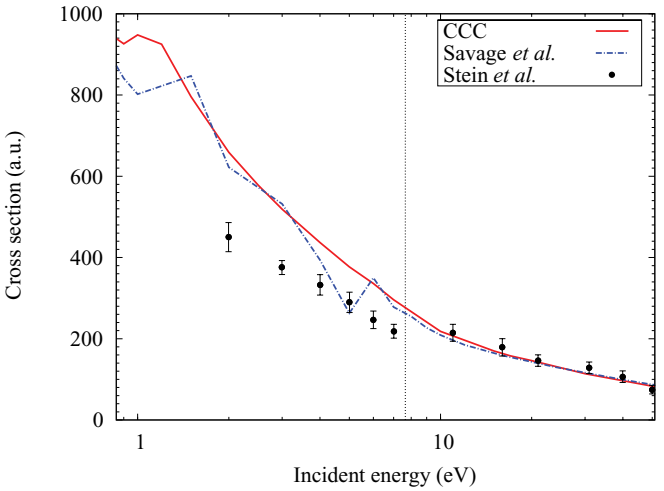

FIG. 4. (Color online) e^+-Mg total scattering cross sections. The vertical line indicates the Mg-ionization threshold. Experimental data are due to Stein *et al.* [2].

Ps states ($n_{\rm Ps} = 0$), and the convergent single-center CCC results of Savage *et al.* [13] indicates the slow convergence rate with increasing $l_{\rm max}$. The reason for such a slow convergence is due to strong coupling to virtual Ps-formation channels, which can be taken into account indirectly by using high orbital momentum states or by explicitly including Ps states into expansions. By comparing the results of CCC(79_3,0) with CCC(79_3,1), we can see the importance of such coupling into virtual Ps-formation channels. It shows that, by adding only one Ps state to a quite small basis, we can get the convergent result.

The results given in Fig. 2 show that the basis CCC(79_3,1) is sufficient to get convergent results. Therefore, furthermore, we use only this basis by adding two more states ($2s$ and $2p$) of Ps when the scattering energy is above their thresholds (5.95 eV). The results are denoted as CCC. The partial-wave summed elastic cross section is shown in Fig. 3. It shows that our results, with two center bases, are in excellent agreement with the results of Savage *et al.* [13] (in their energy range of validity), including the position and magnitude of the p-wave resonance. The agreement between our calculations and the results of Mitroy *et al.* [12] is satisfactory except for the position and magnitude of the p-wave resonance.

Figure 4 shows the total scattering cross section above the Ps-formation threshold compared with the single-center results of Savage *et al.* [13] and with the experimental data of Stein *et al.* [2]. Below the Ps-formation threshold, the results are the same as in Fig. 3. Between the Ps-formation and the ionization thresholds, our results are above the experimental data of Stein *et al.* [2]. The single-center calculations of Savage *et al.* [13] were not valid in this energy region and did not produce convergent results. Above 10 eV, our results compare well with results of the single-center CCC and the experimental data.

The Ps-formation cross section is presented in Fig. 5. Our results are compared with the previous calculations of Gribakin and King [6], Hewitt *et al.* [9], Walters (data taken from Ref. [3]), and Cheng and Zhou [11]. Also presented are experimental data of Surdutovich *et al.* [3], which are preliminary estimations for the upper and lower limits of the Ps-formation cross sections. Our results compare well qualitatively with the results of the many-body theory by Gribakin and King [6], the close-coupling calculations of Walter as presented by Surdutovich *et al.* [3], and the momentum space optical potential method by Cheng and Zhou [11]. The many-body theory results [6] have been obtained as a nonelastic cross section, and at this energy range, the Ps formation is a dominant contributor. The results of Hewitt *et al.* [9], obtained using only a few Mg and Ps states, are much lower than our results. Quantitative agreement between the given theories is not very satisfactory. Unfortunately, the available experimental data are also reported as preliminary and cannot discriminate the theoretical results as all lie between the lower and the upper limits of the experimental estimations.

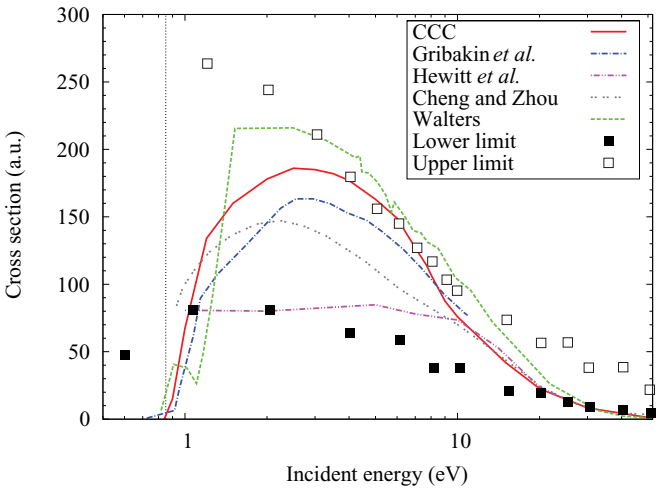

FIG. 5. (Color online) e^+-Mg Ps-formation cross sections. Experimental data for upper and lower limits of Ps-formation cross sections are due to Surdutovich *et al.* [3]. The vertical line indicates the position of the Ps-formation threshold. Other details are given in the text.

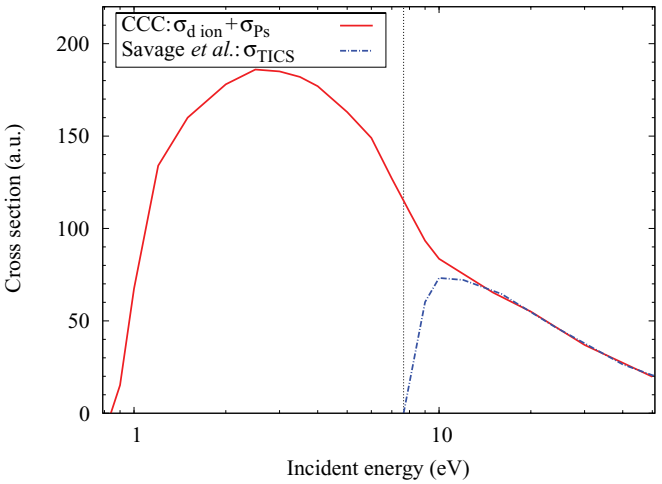

FIG. 6. (Color online) e^+-Mg total ionization cross sections. $\sigma_{d\ ion}$, σ_{Ps}, and σ_{TICS} are direct ionization, Ps-formation, and total ionization cross sections, respectively. The vertical line indicates the Mg-ionization threshold.

Figure 6 shows the total ionization cross section (TICS), which is the sum of the Ps-formation and direct ionization cross sections. The single-center CCC can obtain the TICS above the ionization threshold as a capture to positive pseudostates and cannot separate Ps formation from it. In the two-center approach, cross sections for Ps formation and direct ionization are calculated separately and then are summed up to obtain the TICS. As can be seen from the figure, the two methods agree soon after the ionization threshold, giving us great confidence in the accuracy of the presented results.

IV. CONCLUSION

The CCC approach has been applied to positron scattering on magnesium explicitly including the Ps-formation channels. The importance of the Ps channels, even below the Ps-formation threshold, has been demonstrated by showing that the single-center CCC results can be reproduced with relatively small bases if one Ps state is included. Using the two-center method, we obtained the Ps-formation cross section, which is in qualitative agreement with previous theories and preliminary experimental estimations. More accurate measurements of elastic cross sections at low energies and Ps-formation cross sections would be of interest, and we hope it will be possible in the near future. Our future outlook is to extend the code for positron scattering on noble gases.

ACKNOWLEDGMENTS

The work was supported by the Australian Research Council. We are grateful for access to the Australian National Computing Infrastructure (NCI) Facility and its Western Australian node iVEC.

[1] T. S. Stein, J. Jiang, W. E. Kauppila, C. K. Kwan, H. Li, A. Surdutovich, and S. Zhou, Can. J. Phys. **74**, 313 (1996).
[2] T. S. Stein, M. Harte, J. Jiang, W. E. Kauppila, C. K. Kwan, H. Li, and S. Zhou, Nucl. Instrum. Methods Phys. Res. B **143**, 68 (1998).
[3] E. Surdutovich, M. Harte, W. E. Kauppila, C. K. Kwan, and T. S. Stein, Phys. Rev. A **68**, 022709 (2003).
[4] R. Szmytkowski, J. Phys. II **3**, 183 (1993).
[5] R. I. Campeanu, R. P. McEachran, L. A. Parcell, and A. D. Stauffer, Nucl. Instrum. Methods Phys. Res. B **143**, 21 (1998).
[6] G. F. Gribakin and W. A. King, Can. J. Phys. **74**, 449 (1996).
[7] G. G. Ryzhikh, J. Mitroy, and K. Varga, J. Phys. B **31**, 3965 (1998).
[8] M. W. J. Bromley, J. Mitroy, and G. Ryzhikh, J. Phys. B **31**, 4449 (1998).
[9] R. N. Hewitt, C. Noble, B. H. Bransden, and C. J. Joachain, Can. J. Phys. **74**, 559 (1996).
[10] C. P. Campbell, M. T. McAlinden, A. A. Kernoghan, and H. R. J. Walters, Nucl. Instrum. Methods Phys. Res. B **143**, 41 (1998).
[11] C. Cheng and Y. Zhou, Phys. Rev. A **73**, 024701 (2006).
[12] J. Mitroy, J. Y. Zhang, M. W. J. Bromley, and S. I. Young, Phys. Rev. A **78**, 012715 (2008).
[13] J. S. Savage, D. V. Fursa, and I. Bray, Phys. Rev. A **83**, 062709 (2011).
[14] D. V. Fursa and I. Bray, J. Phys. B **30**, 5895 (1997).
[15] D. V. Fursa and I. Bray, Phys. Rev. A **63**, 032708 (2001).
[16] I. Bray, Phys. Rev. A **49**, 1066 (1994).
[17] J. B. Furness and I. McCarthy, J. Phys. B **6**, 2280 (1973).
[18] R. Utamuratov, A. S. Kadyrov, D. V. Fursa, I. Bray, and A. T. Stelbovics, J. Phys. B **43**, 125203 (2010).
[19] A. S. Kadyrov and I. Bray, Phys. Rev. A **66**, 012710 (2002).
[20] I. H. Sloan and E. J. Moore, J. Phys. B **1**, 414 (1968).
[21] A. V. Lugovskoy, A. S. Kadyrov, I. Bray, and A. T. Stelbovics, Phys. Rev. A **82**, 062708 (2010).